NASA TECHNICAL NOTE

NASA TN D-5467

NASA TN D-5467

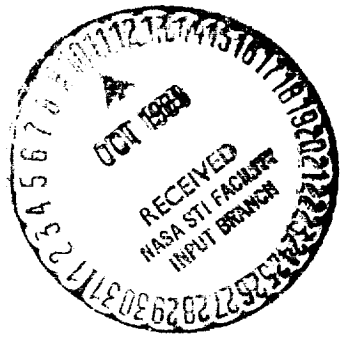

DISCHARGE COEFFICIENTS FOR THICK PLATE ORIFICES WITH APPROACH FLOW PERPENDICULAR AND INCLINED TO THE ORIFICE AXIS

by John E. Rohde, Hadley T. Richards, and George W. Metger

Lewis Research Center
Cleveland, Ohio

NATIONAL AERONAUTICS AND SPACE ADMINISTRATION • WASHINGTON, D. C. • OCTOBER 1969

1. Report No. NASA TN D-5467	2. Government Accession No.	3. Recipient's Catalog No.
4. Title and Subtitle DISCHARGE COEFFICIENTS FOR THICK PLATE ORIFICES WITH APPROACH FLOW PERPENDICULAR AND INCLINED TO THE ORIFICE AXIS		5. Report Date October 1969 6. Performing Organization Code
7. Author(s) John E. Rohde, Hadley T. Richards, & George W. Metger		8. Performing Organization Report No. E-5119
9. Performing Organization Name and Address Lewis Research Center National Aeronautics and Space Administration Cleveland, Ohio 44135		10. Work Unit No. 720-03-00-79-22 11. Contract or Grant No. 13. Type of Report and Period Covered Technical Note
12. Sponsoring Agency Name and Address National Aeronautics and Space Administation Washington, D.C. 20546		14. Sponsoring Agency Code

15. Supplementary Notes

16. Abstract

Experimental discharge coefficients were obtained for thick plate orifices with the approaching flow perpendicular or inclined to the orifice axis. Parameters investigated were temperature and pressure levels; orifice pressure differential; approach Mach number; orifice diameter, thickness, and inlet edge condition; orifice surface finish; interference of multiple orifices; and approach passage geometry and length. The discharge coefficients were found to be dependent on approach Mach number, static pressure differential across the orifice, inlet edge radius on the orifice, angle between the main flow and the axis of the orifice, and the ratio of the orifice thickness to diameter.

17. Key Words (Suggested by Author(s))	18. Distribution Statement
Discharge nozzle coefficient Inclined orifice Orifice Thick-plate	Unclassified - unlimited

19. Security Classif. (of this report)	20. Security Classif. (of this page)	21. No. of Pages	22. Price*
Unclassified	Unclassified	29	$3.00

*For sale by the Clearinghouse for Federal Scientific and Technical Information Springfield, Virginia 22151

DISCHARGE COEFFICIENTS FOR THICK PLATE ORIFICES WITH APPROACH FLOW PERPENDICULAR AND INCLINED TO THE ORIFICE AXIS

by John E. Rohde, Hadley T. Richards, and George W. Metger

Lewis Research Center

SUMMARY

The flow discharged through thick plate orifices with the approaching flow perpendicular or inclined to the orifice axis was experimentally investigated. The study was conducted to determine the influence of the flow and geometric parameters. The parameters investigated were temperature and pressure levels; orifice pressure differential; approach Mach number; orifice diameter, thickness, and inlet edge condition; orifice surface finish; interference of multiple orifices; and approach passage geometry and length.

The discharge coefficients were correlated with a velocity head parameter which consisted of the ratio of the velocity head of the flow through the orifice to the velocity head of the flow approaching the orifice axis for various approach Mach numbers. The discharge coefficients were found to be dependent on the approach Mach number, the static pressure differential across the orifice, the inlet edge radius of the orifice, the angle between the approaching flow and the axis of the orifice, and the ratio of the orifice thickness to orifice diameter. The effects of temperature and pressure levels, orifice surface finish, multiple orifice interference, and approach passage geometry and length on discharge coefficients were found to be negligible for the cases considered.

INTRODUCTION

Knowledge of the flow through thick plate orifices with the approach velocity perpendicular or inclined to the orifice axis is required to predict the performance of some internally cooled turbine blades and vanes. The need for cooled turbine blades and vanes for high performance gas-turbine aircraft engines is well recognized. In order to provide cooled blades or vanes that have high heat transfer effectiveness with a minimum coolant flow, the internal coolant passages become comparatively complex. Thick plate

orifice arrangements are employed in the impingement cooling concept wherein a high velocity jet of cooling air is directed against the inside surfaces of a blade or vane. Thick plate orifices may also be employed in the transfer holes used to supply cooling air to the blade or vane leading and trailing edge regions from a radial midchord passage.

Previous studies of orifice discharge coefficients with the approaching flow perpendicular to the orifice axis are reported in references 1 to 7. References 1 and 2 considered perpendicular inlet flow through relatively thin plate orifices and perforated materials, reference 3 perpendicular velocity on both the inlet and exit faces of the orifice, references 4 to 6 only the perpendicular exit velocity, and reference 7 perpendicular inlet velocities to rectangular holes, step louvers, and scoops.

The basic conclusion of these investigations was that the flow through the orifice is influenced significantly by the inlet velocities perpendicular to the orifice axis and that for low exit velocities perpendicular to the orifice axis and high jet velocity, the effect of exit flow velocity can be eliminated by calculation of a revised exit jet discharge pressure.

In thick plate orifices, orifice thickness is an influential variable to the flow. Reference 1 indicates the influence of the orifice thickness but the work was primarily concerned with thin plate orifices. The orifice flow is further influenced by the geometry of the main flow duct, geometry of the orifice, the flow conditions, and the proximity of other orifices as shown in the thin plate orifice results of references 1, 3, and 7.

The present investigation considered the following parameters: temperature and pressure levels; orifice pressure differential; approach Mach number; orifice diameter, thickness, and inlet edge condition; orifice surface finish; interference of multiple orifices; and approach passage geometry and length. The geometry of the main flow duct in all cases but one was a 0.25-inch (0.063-cm) diameter tube. This tube diameter was representative of a size to be expected in a turbine blade. (The exception was a rectangular cross-section main duct to investigate the effect of curvature of the upstream face of the orifice.) The orifice thickness varied from 0.06 to 0.25 inch (0.15 to 0.63 cm) and the orifice diameters varied from 0.59 to 0.128 inch (0.150 to 0.325 cm). The inlet edge of the orifice was varied from a sharp corner to a 0.030-inch (0.076-cm) radius. The main duct inlet airflow Mach number was varied from 0 to 0.65, static pressure was varied from 20.0 to 80.0 psia (13.8 to 55.2 N/cm^2), and the temperature was varied from ambient to approximately 1000° F (811 K). Orifices with axes at 45° and 90° angles to the main duct flow were investigated.

SYMBOLS

A	flow area
C_d	discharge coefficient, ratio of measured to ideal flow through the orifice
D	hydraulic diameter of the main duct
d	orifice diameter
f	friction factor
g	gravitational conversion factor
L	linear distance between the pressure tap and orifice
M	Mach number
P_T	total pressure in the main duct
p	static pressure
R	gas constant for air
Re	Reynolds number
T	static temperature
T_T	total temperature in the main duct
t	wall thickness
V	velocity
w	measured mass weight of flow
X	entrance length of the main duct
α	inclination angle or the orifice, see fig. 4
γ	specific heat ratio
ρ	density

Subscripts:

d	main duct
j	jet exit
o	orifice

APPARATUS

A schematic diagram of the basic setup utilized for the investigation is shown in figure 1. Air at 125 psig (86.2 N/cm^2) was supplied through a filter and dryer, two pressure regulators in series, a rotameter, air heater, and into the main duct of the test section. Air leaving the main duct and collecting duct (orifice exhaust) was passed through throttling valves and cooling coils to an atmospheric exhaust system with the orifice exhaust passing through an additional rotameter. The air flow rate through the main duct and through the orifice and the static pressures in the main duct and orifice duct were controlled by adjustments of both the upstream and downstream throttling valves. The air heater and dryer and the cooling coils were not in the system during the ambient temperature runs.

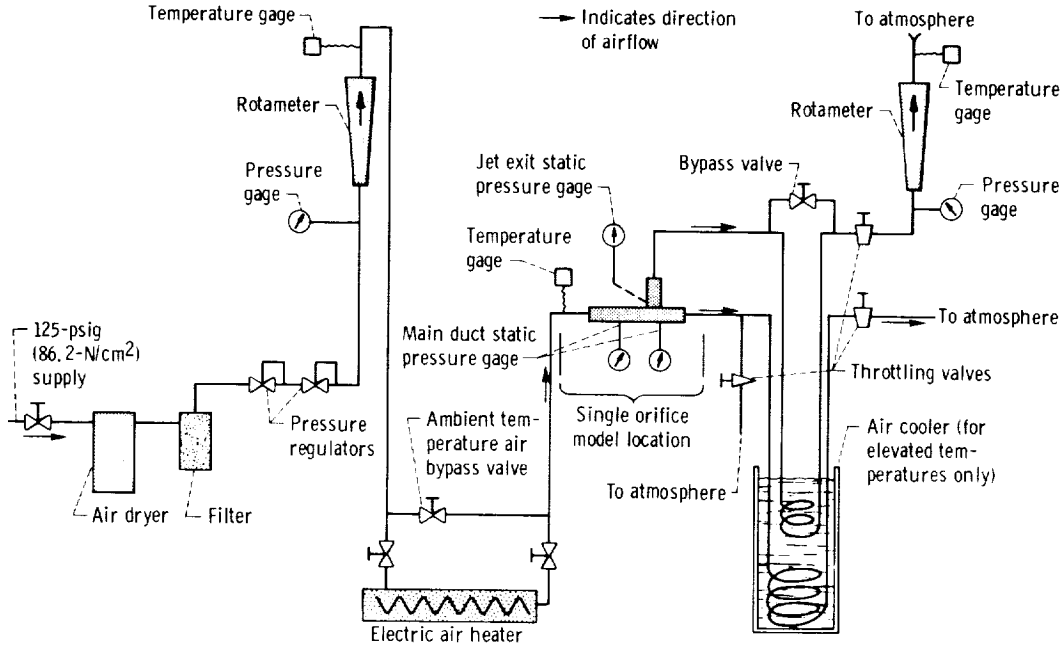

Figure 1. - Single orifice model test setup.

Description of Models

Orifice geometry variations were obtained by the construction of 12 different models. The models were made of brass or stainless steel with the main duct or part of the main duct formed in halves for the majority of models and joined by soft solder or brazing as shown in figure 2. This method of fabrication was employed to allow inspection of the

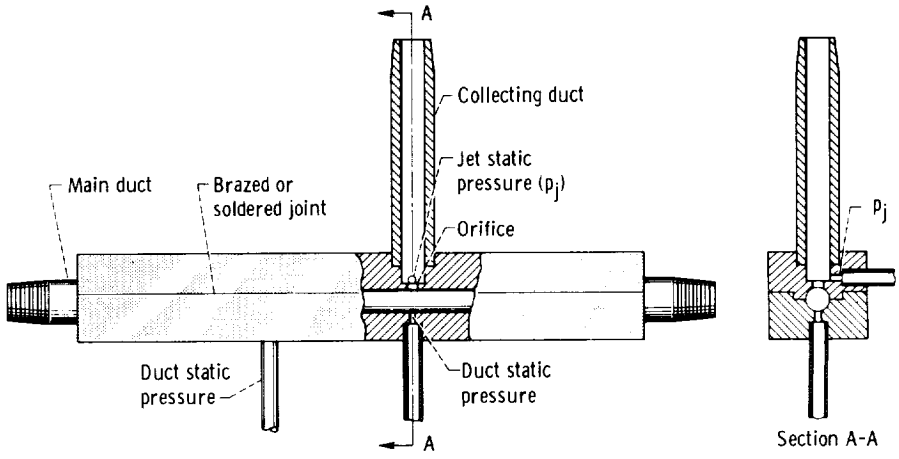

Figure 2. - Typical single orifice model showing split construction.

orifices after final machining and to permit disassembly if necessary. The models were drilled, reamed, and polished with conventional machine tools. The orifice diameter and edge condition were carefully examined and measured with optical instruments and plug gages. Each of the standard models had a nominal upstream duct entrance length of 3.5 inches (8.89 cm) and a diameter of 0.25 inch (0.63 cm), resulting in a length to diameter ratio of 14. This standard X/D of 14 produces fully developed flow for the turbulent flow which existed in the main duct of the models. To determine the entrance effect of the developing boundary layer, one of the models was constructed so that it could be tested with a length to diameter ratio of 2 or 14 depending on the end used as the inlet. This model is shown in figure 3. In addition to the models with a circular main duct, one

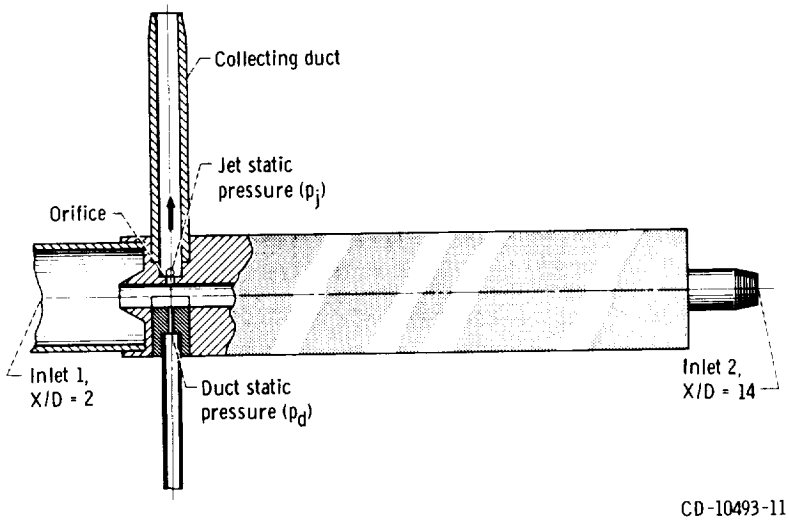

Figure 3. - Single orifice model 5 designed for two length to diameter ratios.

model was constructed of a rectangular duct to determine the effect of main duct curvature. This same model was modified after initial testing by machining a radius on the upstream orifice edge. Inspection of radius and additional testing was then carried out. Figure 4 describes model 9, which was the only model with an orifice axis inclined to the main stream. The angle α (indicated in the figure) was equal to 45°.

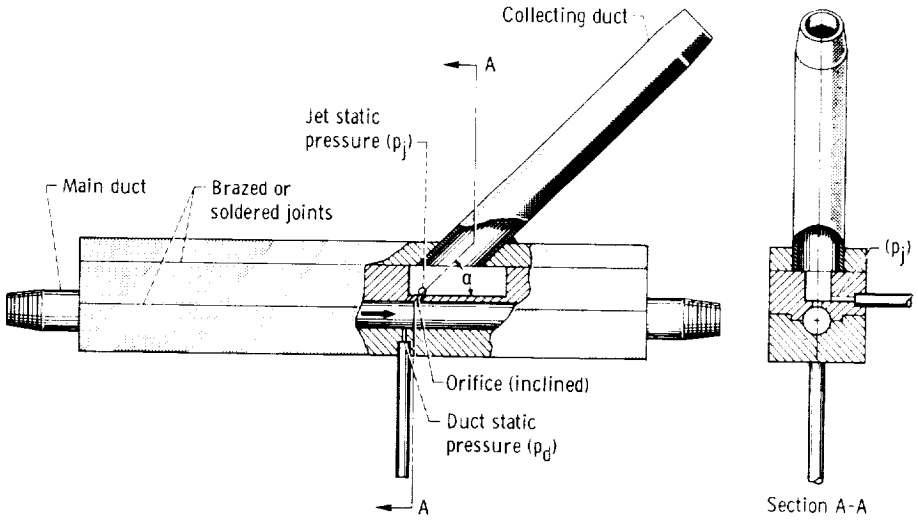

Figure 4. - Inclined orifice model 9.

Since all of the models described above were carefully made (reamed, lapped, and polished) and inspected, it was decided to simulate a production orifice by electrical discharge machining orifices in a representative number of models. Four duplicate models for each of two different sizes (i.e., a total of eight models) were fabricated by this process.

Table I identifies each of the models considered in this investigation. The table identifies the models by number and summarizes the pertinent dimensional characteristic associated with each. The accuracy in measuring the orifice diameter was ±0.0005 inch (0.0013 cm).

TABLE I. - MODEL CONFIGURATIONS INVESTIGATED, INCLUDING PERTINENT DIMENSIONS

Model	Ratio of wall thickness to orifice diameter, t/d	Orifice diameter, d		Wall thickness, t		Description
		in.	cm	in.	cm	
1	0.51	0.1277	0.3244	0.065	0.165	Steel
2	1.02	.0635	.1613	.065	.165	Steel
3	1.05	.0630	.1600	.066	.168	Split brass
4	1.60	.0601	.1526	.096	.244	Split brass
5	2.00	.0630	.1600	.126	.320	Split brass, X/D = 2 or 14
6	2.83	.0660	.1676	.187	.475	Steel
7	4.00	.0618	.1570	.247	.627	Brass
8	1.06	.0615	.1562	.065	.165	Brass, rectangular duct
9	1.01	.0665	.1689	.067	.170	Brass, $\alpha = 45^{\circ}$
[a]10	1.49	.0639	.1623	.095	.241	Steel, orifice EDM[b]
[a]11	.52	.1260	.3200	.065	.165	Steel, orifice EDM[b]
12	1.00	.0590	.1499	.059	.150	Brass, two orifices in tandem

[a]Average dimensions.
[b]Electrical discharge machined.

Test Set-Up and Instrumentation

The basic measurements are shown in figure 1.

(1) Flow rate at the entrance to the main duct

(2) Flow rate through the orifice

(3) Main duct static pressure at a point opposite the orifice

(4) Static pressure at the exit plane of the orifice

(5) Total temperature of the supply air

The main duct static pressure was measured at a point opposite the orifice in most cases. This location was selected because it provided a pressure close to the orifice inlet. Model 1, Model 2, and Model 12 were instrumented with additional pressure taps located up to 1.75 inches (4.45 cm) upstream of the orifice. These additional taps were added to determine any variations in main duct static pressure with flow through the orifice. The position of the static pressure tap at the exit plane was located in the wall of the collecting duct as shown in figure 2 This jet static tap location was selected as close to the exit plane of the orifice as feasible and perpendicular to the axis of the orifice. The total temperature of the supply air was measured by a thermocouple at the rotameter exit when ambient temperature air was used. The heated air total temperature of the

supply air was measured by a shielded thermocouple approximately 10 inches (25.4 cm) upstream of the orifice location. The length of pipe between the heater exit and the orifice was fully insulated to prevent heat losses.

A measurement of the main duct total pressure was not attempted because of the size limitations in the main duct. The total pressure was calculated based on compressible flow relations.

PROCEDURE

Experimental

Three types of tests were made: (1) constant main duct Mach number, (2) all the flow passing through the orifice, and (3) constant pressure differential across the orifice. In the majority of tests the static pressure in the main duct opposite the orifice was maintained at a value of approximately 40 psia (27.6 N/cm^2).

In the constant main duct Mach number tests, the supply air weight flow and static pressure opposite the orifice were maintained constant (constant main duct P_T). The orifice exit pressure was varied in small increments from the main duct static pressure to beyond critical by reducing it to atmospheric. The main duct Mach number was set at nominal values of Mach number between zero and 0.55 for this series of tests.

Tests with all the flow passing through the orifice were made in the same manner as the constant Mach number tests except that all the supply air passed through the orifice. No supply rotameter was needed, and the main duct exit was closed. The main duct static pressure opposite the orifice was maintained constant and the orifice pressure differential was varied as in the constant Mach number runs.

Constant orifice pressure differential ($p_d - p_j$) runs, with a variable main duct Mach number, were made on Model 3. In this case, the orifice pressure differential and main duct static pressure were maintained at constant values and the approach Mach number (and main supply air weight flow) were varied over the maximum range possible.

In some cases, the models were run by first increasing and then decreasing orifice flow. This test procedure was followed in an attempt to detect any hysteresis effect between the orifice flow and the orifice pressure differential. None was detected.

ANALYSIS

The orifice discharge coefficient is defined as the ratio of the actual flow to ideal flow.

$$C_d = \frac{w_o}{\rho_j V_j A_o} \tag{1}$$

The values of the ideal jet velocity and density were determined through the use of the following compressible flow relations:

$$V_j = \sqrt{\frac{2\gamma g R T_T}{(\gamma - 1)} \left[1 - \left(\frac{p_j}{P_T}\right)^{\gamma - 1/\gamma}\right]} \tag{2}$$

$$\rho_j = \frac{p_j}{R T_T} \left(\frac{P_T}{p_j}\right)^{\gamma - 1/\gamma} \tag{3}$$

The equations utilize the pound-mass and pound-force system of units.

In the preceding, the jet velocity is limited to sonic velocity. This limit exists because the orifice does not contain a divergent section to permit supersonic flow.

In the calculation of the ideal jet velocity, the main duct total pressure was used as the total pressure in the jet. The main duct static pressure is a more reasonable value of reference pressure for the case of the approach flow perpendicular to the orifice axis (no velocity head pressure recovery). However, the use of the main duct total pressure as a reference pressure, allows the continuation of the same reference when the orifice is inclined (some of the velocity head is recovered). The use of the main duct total pressure as a reference with the flow perpendicular to the orifice axis gives a slightly higher value of ideal jet velocity.

The main duct total pressure can be determined from the measured static pressure, total temperature, and weight flow by an iterative procedure using the following equations:

$$P_T = p_d \left[1 + \left(\frac{\gamma - 1}{2}\right) M_d^2\right]^{\gamma/\gamma - 1}$$

$$M_d = \frac{V_d}{\sqrt{\gamma g R T_d}}$$

$$V_d = \frac{w_d}{A_d \rho_d}$$

$$\rho_d = \frac{p_d}{RT_d}$$

$$T_d = \frac{T_T}{\left[1 + \left(\frac{\gamma - 1}{2}\right) M_d^2\right]}$$

The measured main duct static pressure opposite the orifice was found to be a function of the flow through the orifice for the models containing the larger diameter orifice and the two orifices acting in tandem. It was determined that the influence of the orifice flow on the main duct static pressure persisted only up to 2 diameters upstream.

When the static pressure measurement opposite the orifice was influenced by the flow through the orifice, the following procedure was employed: The static pressure was measured at a point at least 4 main duct diameters upstream of the orifice, where the static pressure was not influenced by the flow through the orifice. From this static pressure a total pressure was calculated upstream of the orifice as discussed previously. This total pressure was extrapolated downstream by the adiabatic flow in a constant area duct with friction. The following equations from reference 8 were employed for this purpose:

$$-d(p_d) = 2\rho_d \frac{V_d^2 fL}{Dg} + \frac{\rho_d V_d^2 \, d(V_d)}{V_d g}$$

$$\frac{1}{\sqrt{f}} = 4 \log\left(Re_d \sqrt{f}\right) - 0.40$$

RESULTS AND DISCUSSION

Correlation of Data

The discharge coefficient data in this report are presented as a function of the ratio of velocity head of the orifice jet to the velocity head in the main duct, $(P_T - p_j)/(P_T - p_d)$, for constant values of main duct Mach number. This ratio will be called "velocity head ratio" in this report. This kind of plot permits correlation of data for a wide range of gas temperature levels. The method of data presentation is similar to that used in reference 1, except that reference 1 presented data for constant main duct

velocity. The constant main duct velocity correlation does not hold for a wide range of gas temperatures.

Figure 5 shows a plot of discharge coefficient against the velocity head ratio for model 1, the model with the largest diameter orifice (smallest t/d ratio). For this fig-

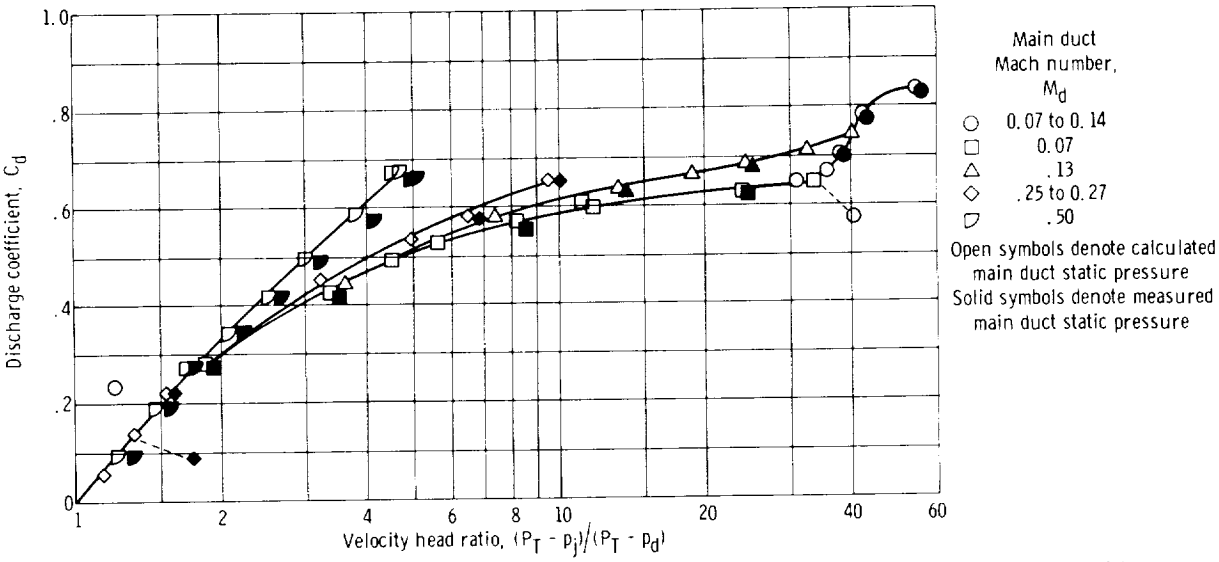

Figure 5. - Effect of main duct static pressure determination on calculated discharge coefficients. Model 1; wall thickness to orifice diameter ratio, 0.51.

ure the static pressure in the main duct opposite the orifice was determined by two different methods: (1) it was measured directly, and (2) it was calculated by compressible flow friction pressure drop relations and a measured upstream static pressure. In both cases the main duct total-pressure was then calculated from the static pressure, total temperature, and weight flow rate. Figure 5 shows the error introduced by using the measured static pressure opposite the orifice (which is influenced by the orifice flow) is small. For all the other models (which had smaller orifices), except the model with two orifices in parallel (model 12), this pressure correction was insignificant and was not employed.

Figure 5 shows that the data for various main duct Mach numbers tend to form a common curve at lower values of velocity head ratio (usually lower values of orifice flow). At the higher values of velocity head ratio separate curves are obtained for each main duct Mach number. The upper end of the curves cover the region where the velocity in the jet reaches the speed of sound. The flow through an orifice can continue to increase after sonic velocity is reached in the jet as explained in reference 9. An orifice first has sonic velocity occurring at the vena contracta. Unlike a flow nozzle, the orifice flow with sonic velocity at the vena contracta is affected by reductions in the downstream pressure. The reduction in the downstream pressure causes the vena contracta to open up and allow

more flow to pass through the orifice. This opening in the vena contracta continues until the jet completely fills the orifice and the orifice chokes the flow.

Effects of Main Duct Mach Number and Pressure Ratio Across Orifice

The individual effects of main duct Mach number and pressure ratio across the orifice are difficult to determine from the correlation shown in figure 5. Because of this difficulty, figure 6 is presented to show the discharge coefficient against the main duct approach Mach number for a typical configuration and for three different constant orifice pressure ratios. The discharge coefficient shown decreases with increased main duct Mach number and increases with increased pressure ratio across the orifice. Similar trends were noted in the discharge coefficients of all the other models investigated.

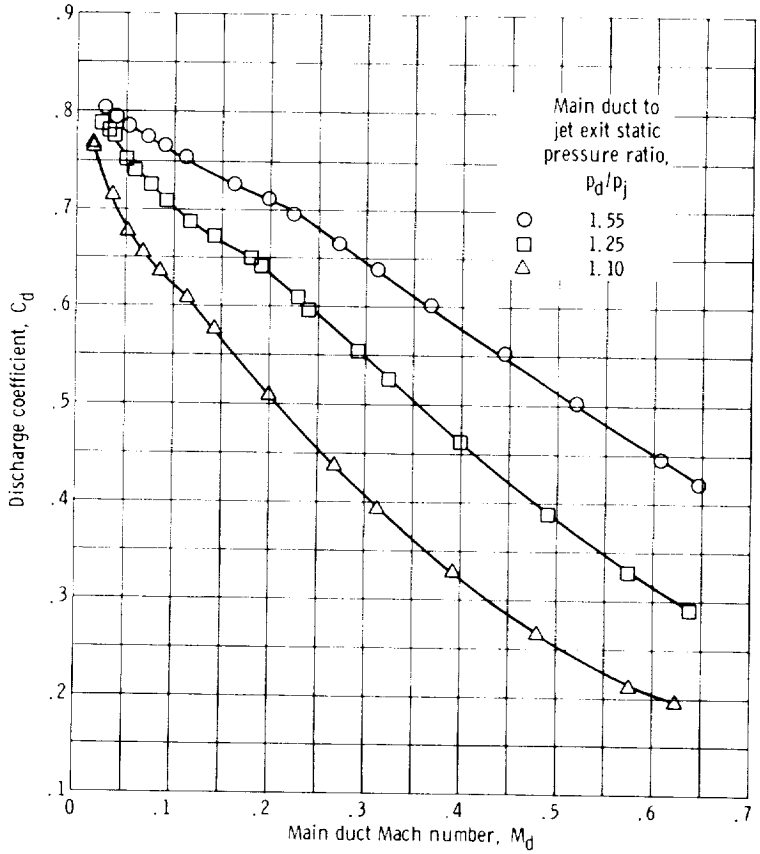

Figure 6. - Effect of main duct Mach number and pressure ratio on orifice discharge coefficient. Model 3; wall thickness to orifice diameter ratio, 1.05; main duct static pressure, 38.7 psia (26.7 N/cm^2).

Effect of Wall Thickness and Orifice Diameter

The discharge coefficient is a function of the static pressure at the orifice exit. Consider the static pressure variation along an ideal vena contraction at the entrance of a straight tube with friction. The ideal vena contraction will have a static pressure variation which is a function of t/d, and the static pressure variation in the tube is also a function of t/d. Therefore, the discharge coefficient will be a function of the t/d ratio.

The correlation of the data for orifices with a t/d from 1.05 to 4.00 is shown in figure 7, and data for t/d = 0.51 is shown in figure 5. The data in figure 7 correlate in the same manner as explained for figure 5. The data points located on the far right of the figure and separated from the other data points, represent the discharge coefficient for the case where all the flow passes through the orifice.

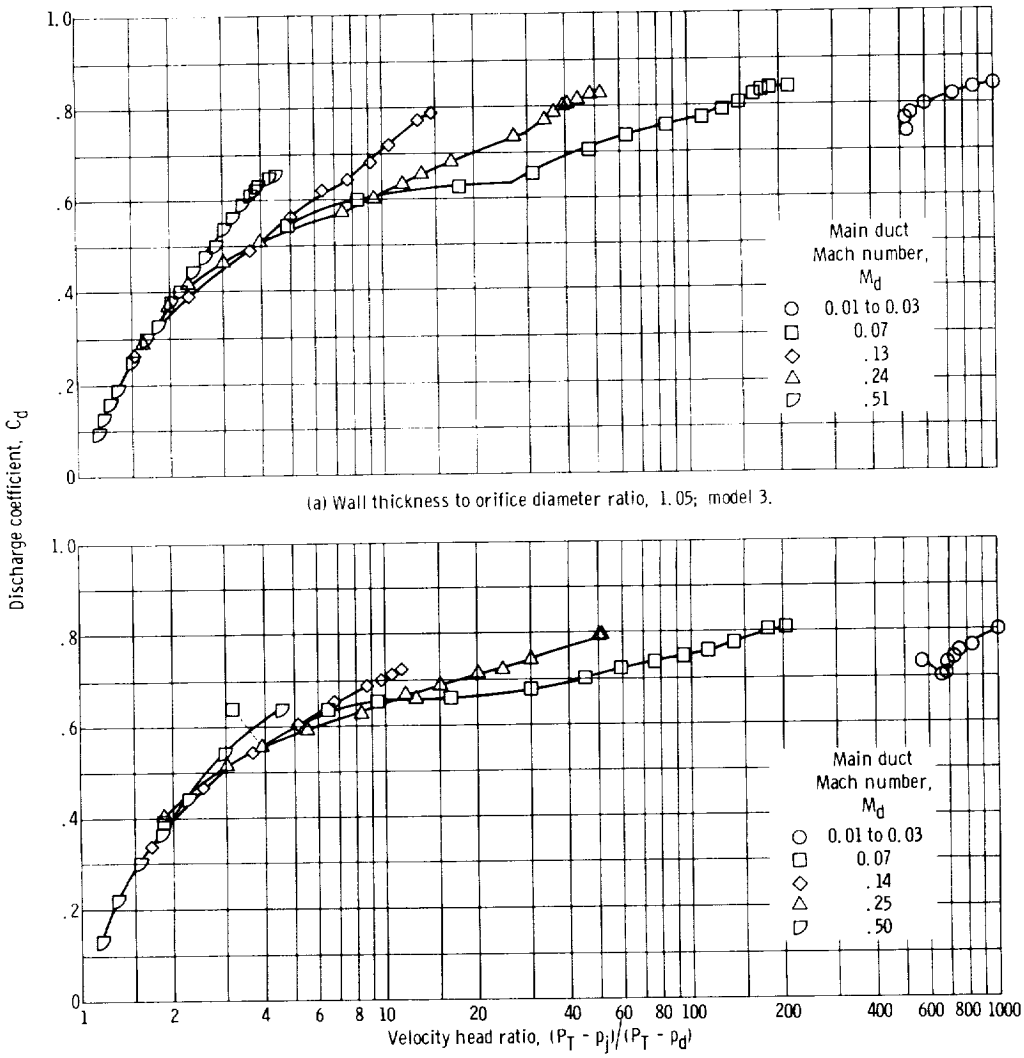

(a) Wall thickness to orifice diameter ratio, 1.05; model 3.

(b) Wall thickness to orifice diameter ratio, 1.60; model 4.

Figure 7. - Effects of velocity head ratio and main duct Mach number on orifice discharge coefficient.

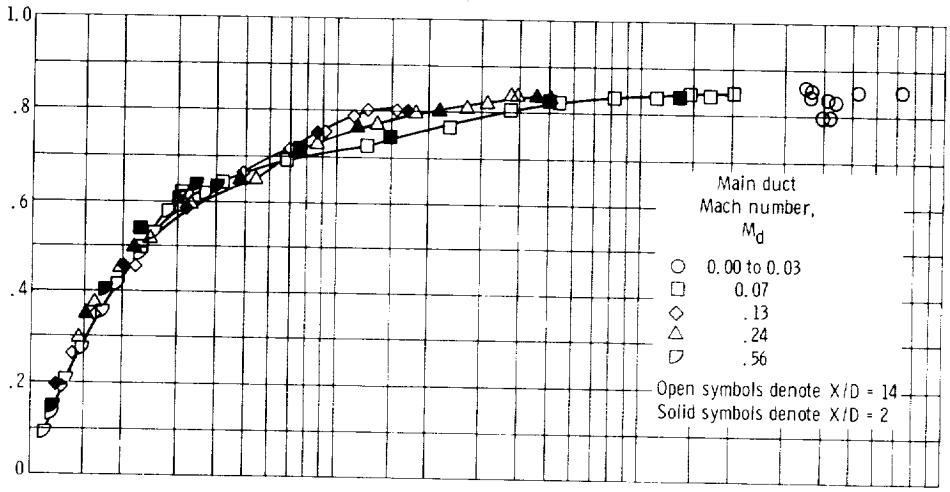

(c) Wall thickness to orifice diameter ratio, 2.00; model 5.

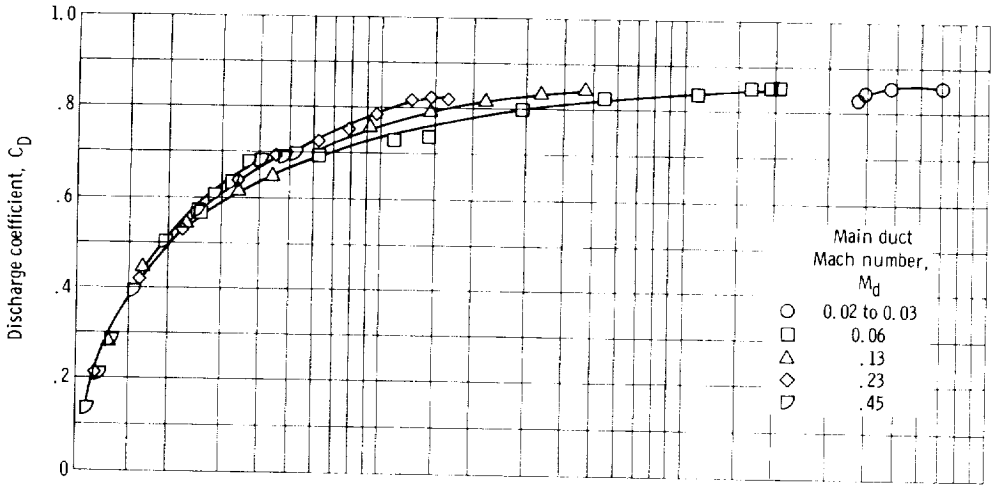

(d) Wall thickness to orifice diameter ratio, 2.83; model 6.

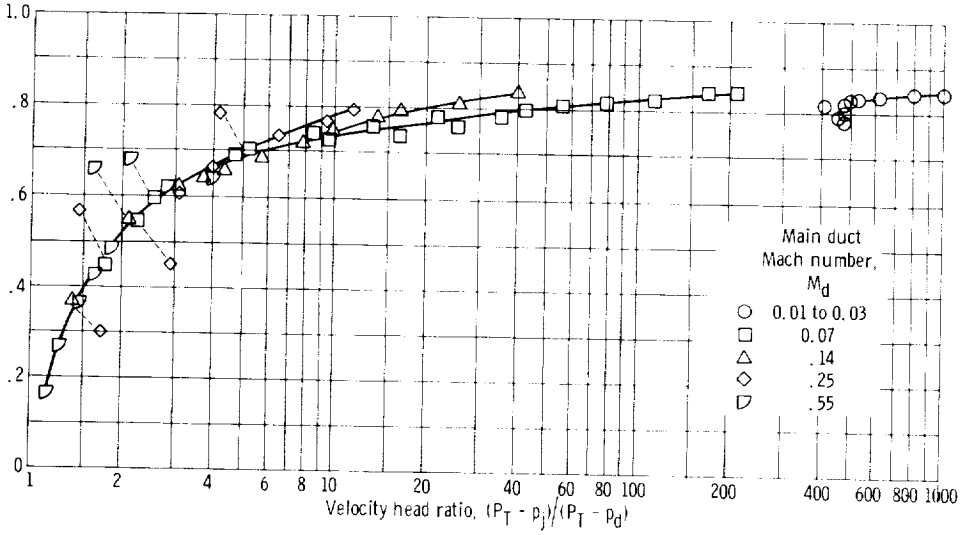

(e) Wall thickness to orifice diameter ratio, 4.00; model 7.

Figure 7. - Concluded.

Figure 8 is a composite of data taken from figures 5 and 7 and reference 1 for a main duct Mach number of 0.13 to 0.14. Similar figures can be constructed for other main duct Mach numbers if desired. The data from this investigation show that at the lower velocity head ratios the discharge coefficient increases with increasing t/d ratio for a t/d less than 4.00. At the higher values of velocity head ratio, the frictional pressure drop starts to reduce the discharge coefficient with increasing t/d ratio. At the lower values of velocity head ratio the discharge coefficient curve for t/d = 2.83 is lower than the curve for t/d = 4.00. However, at the higher values of velocity head ratio the above discharge coefficient curves cross and the curve for a t/d = 2.83 is higher than the curve for a t/d = 4.00.

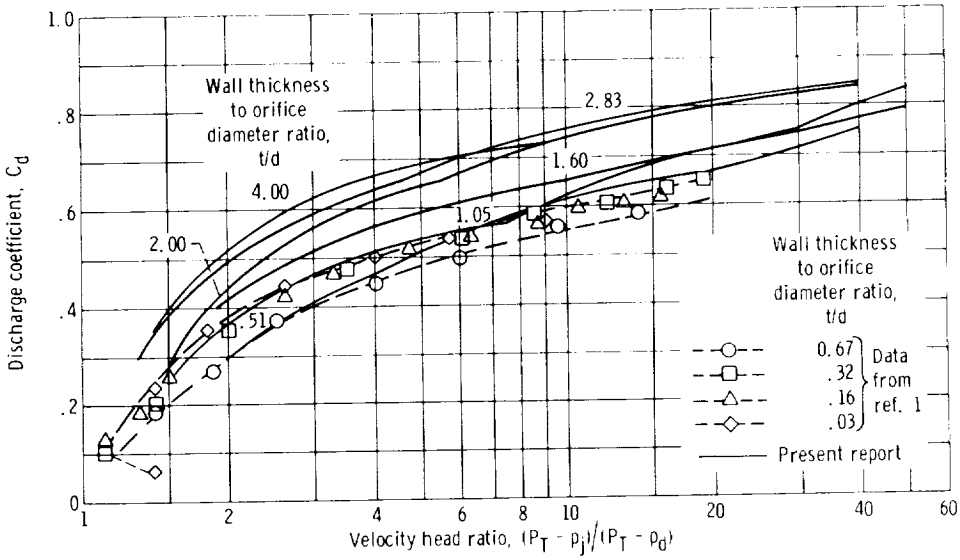

Figure 8. - Comparison of discharge coefficients for various orifices at constant main duct Mach number of 0.13 to 0.14.

However, the results of reference 1 for a t/d less than 0.67, indicate that the discharge coefficient will decrease with increasing t/d ratio. This variation can be explained, if one considers the relative motion of the vena contracta with respect to the orifice exit plane. In the thin plate orifices the vena contracta or point of minimum static pressure occurs downstream of the orifice exit (or pressure tap). As the t/d of the orifice increases, this vena contracta moves upstream past the orifice exit. With the vena contracta located upstream of the orifice exit, some expansion of the jet occurs before the orifice exit plane is reached. These variations in vena contracta location, and hence the measured exit pressure, produce the variations in C_d with t/d ratio.

Comparison of the curves for a t/d ratio of 0.51 with the t/d ratio of 0.67 of reference 1, indicates that the t/d = 0.67 has a slightly lower discharge coefficient when

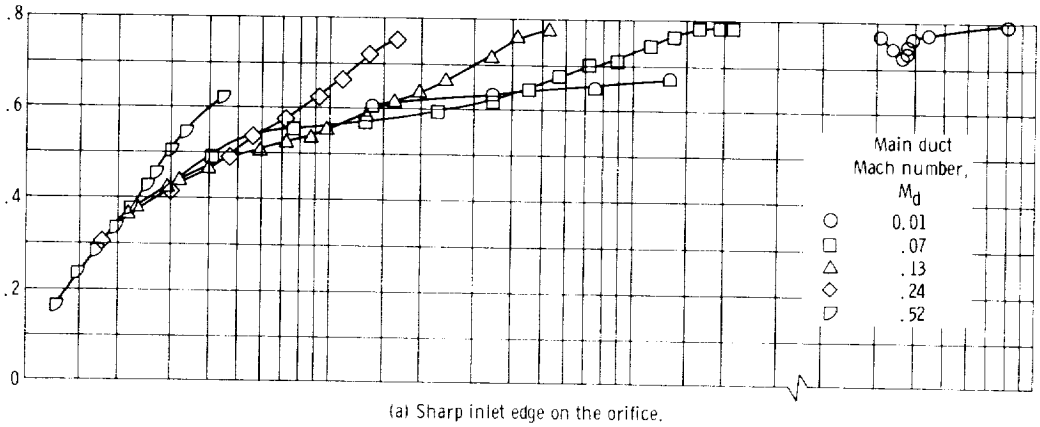

(a) Sharp inlet edge on the orifice.

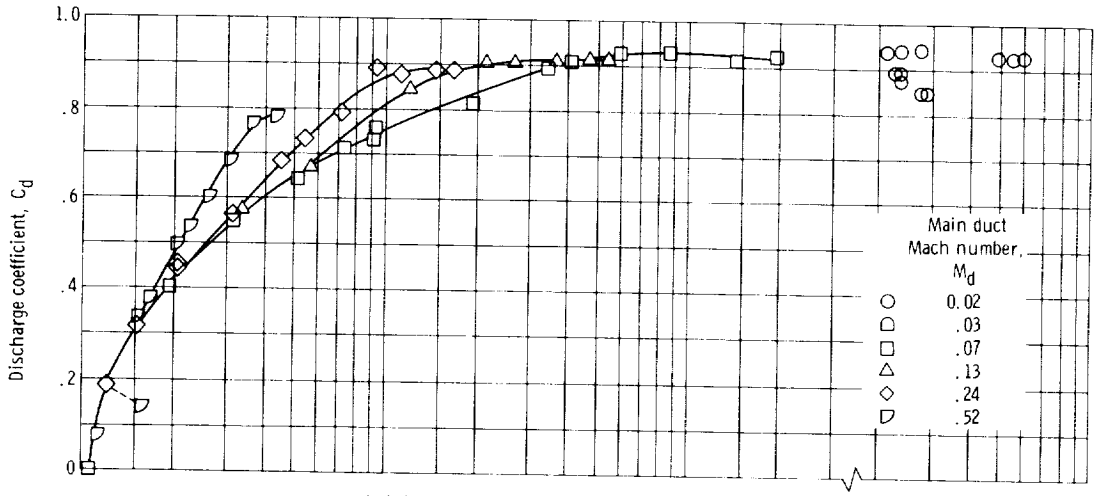

(b) Inlet edge radius of 0.012 inch (0.030 cm) on orifice.

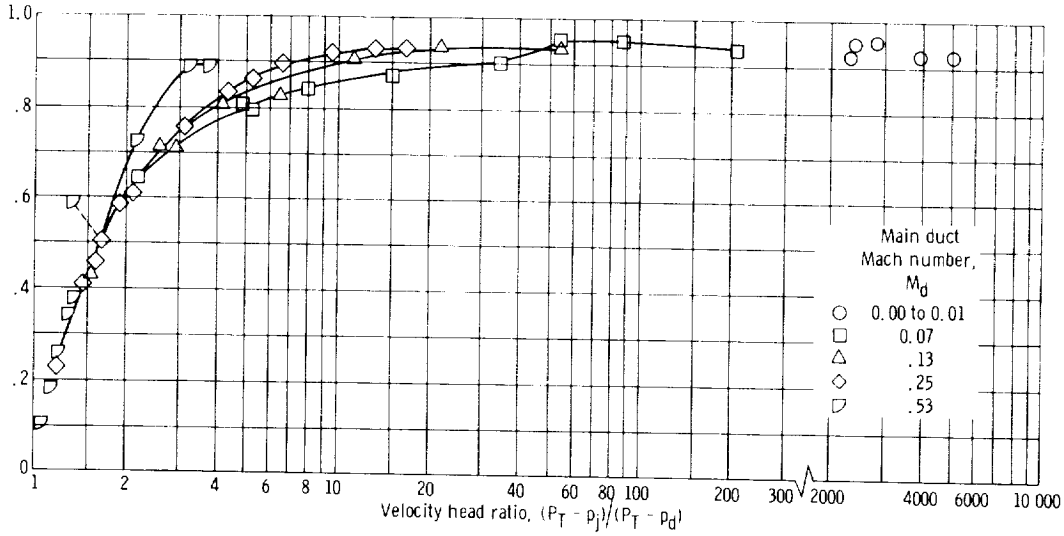

(c) Inlet edge radius of 0.030 inch (0.076 cm) on orifice.

Figure 9. - Variation of orifice discharge coefficient from rectangular main duct for several main duct Mach numbers. Wall thickness to orifice diameter ratio, 1.06; model 8.

it should have a larger value. This slight variation in discharge coefficient can be attributed to the fact that the data of reference 1 were taken with a circular orifice in a square duct rather than a circular main duct. It will be shown later that the variation in discharge coefficient from a circular main duct to a rectangular main duct produces this same decrease in discharge coefficient.

Reference 10 showed that the discharge coefficient is dependent on the ratio of orifice thickness to diameter when t/d is greater than 0.5 for the case of flow parallel to the orifice axis. The variation indicated was that the discharge coefficient increased from 0.61 with increasing t/d ratios to a maximum of 0.81 at a t/d of approximately 2 and then started to decrease at t/d greater than 2. Figure 8 indicates the same general trend for the case of the approach flows perpendicular to the orifice with a maximum occurring somewhere near a t/d of 2.83 for the higher orifice flow (upper end of the curve).

Effect of the Inlet Edge Condition of the Orifice

The orifices in the models reported in figures 5 and 7 all contained an initially sharp inlet edge. The model reported in figure 9 contained an initially sharp inlet edge orifice which was later modified to a 0.012-inch (0.030-cm) radius and then to a 0.030-inch (0.076-cm) radius on the inlet edge.

Figure 10 shows a composite of the three inlet edge conditions at one main duct Mach number. This figure shows that a significant increase in discharge coefficient is obtained by rounding the inlet edge. The larger inlet radius causes the discharge coefficient to increase to as high as 0.94, nearly the value of a flow nozzle discharge coefficient. The

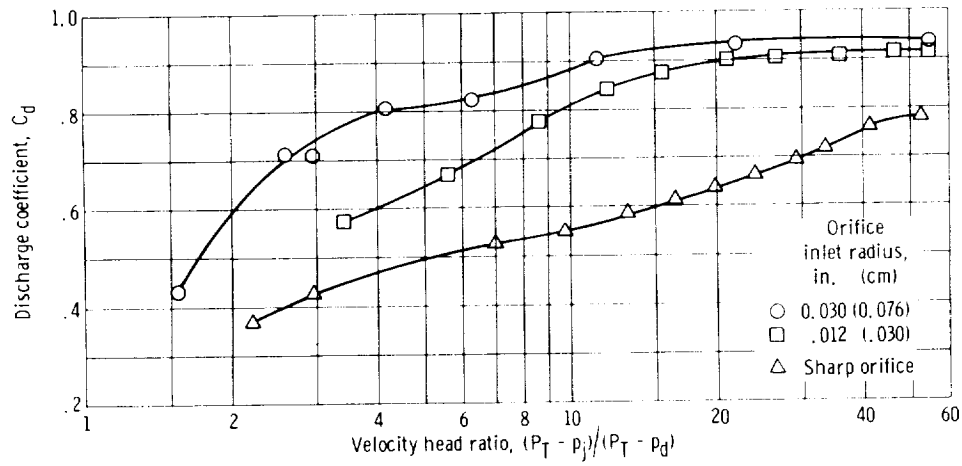

Figure 10. - Variation of orifice discharge coefficient with orifice inlet radius condition. Wall thickness to orifice diameter ratio, 1.06; model 8; main duct Mach number, 0.14.

increase in the discharge coefficient is caused by a reduction or elimination of the separation at the upstream inlet edge.

Effect of Inclined Orifice Axis

The orifice axes in the models (figs. 5, 7, and 9) were all perpendicular to the main duct flow; for one model, the orifice was placed at a 45° angle to the main duct flow in model 9 (shown in fig. 4). Figure 11 shows model 9 and for comparison a band of the

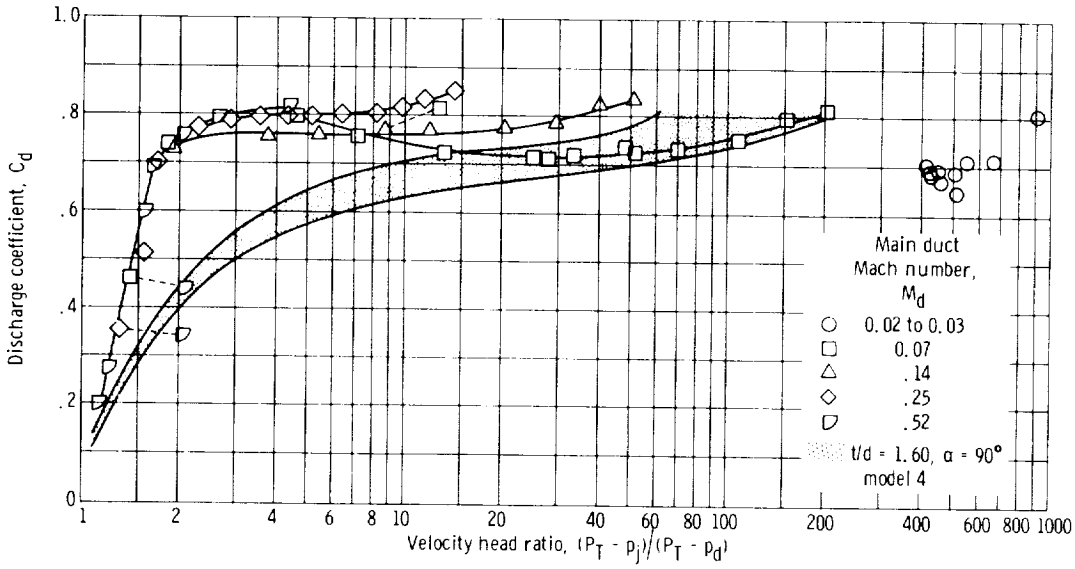

Figure 11. - Effect of inclining orifice axis to main duct axis on discharge coefficient with perpendicular axis model included for comparison. Wall thickness to orifice diameter ratio, 1.01; inclination angle, 45 ; model 9.

data for model 4 with a t/d ratio 1.6 and $\alpha = 90^{\circ}$. For model 9 the wall thickness to diameter ratio was 1.01, but the orifice bore length on the angle to diameter ratio was 1.43. The figure shows the significantly higher values of discharge coefficient obtained by slanting the orifice relative to the direction of flow in the duct. This increase in flow can be attributed to the main stream velocity head, which the orifice "sees" when tilted. It should be observed that the discharge coefficient remains fairly constant over a considerable range of velocity head ratio.

Effect of Main Duct Wall Curvature

Figure 12 shows a comparison of data for models 3 and 8. Both have a t/d equal to

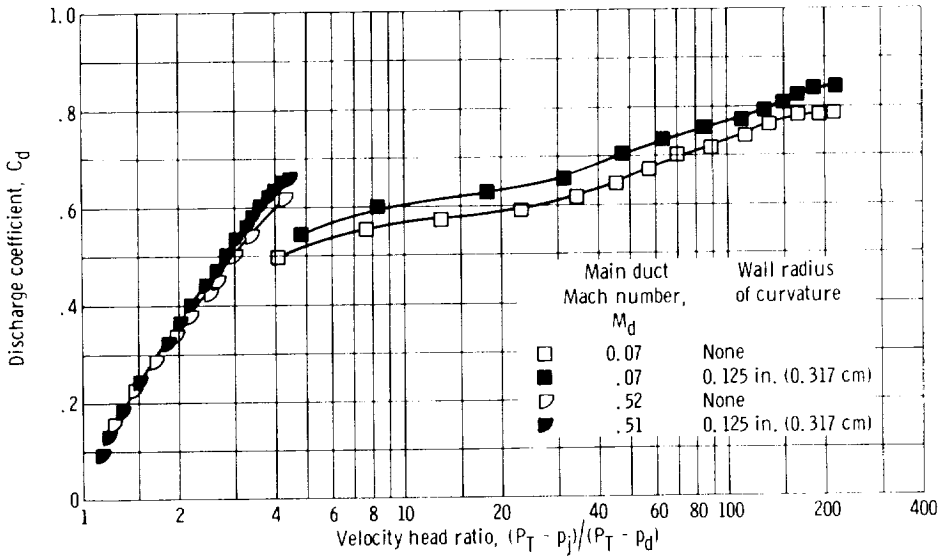

Figure 12. - Effect of main duct wall curvature on orifice discharge coefficient. Model 8 wall thickness to orifice diameter ratio, 1.06; model 3 wall thickness to orifice diameter ratio, 1.05.

1.0 but model 8 has a 1/2- by 1/4-inch (1.27- by 0.64-cm) rectangular cross-section main duct as mentioned previously. Discharge coefficients are consistently higher for model 3. The curvature of the orifice surface (acting as convergent inlet) could decrease the turning of the air when passing through the orifice. The decreased turning would allow a larger vena contracta to exist. Also, the secondary flow in the rectangular duct could cause a decrease in the discharge coefficient.

Pressure Effect

Orifice discharge coefficients for a range of main duct Mach numbers and static pressure p_d are plotted in figure 13. The main duct static pressure levels employed were 20, 40, 60, and 80 psia (13.8, 27.6, 41.4, and 55.2 N/cm^2). The figures show a slight variation of the discharge coefficient at the higher pressure. The use of the 80 psia pressure level required a variation in the instrumentation which could contribute to the slight variation noted. However, even with this slight variation, the lower pressure values are adequate for design purposes at higher pressures. This same insensitivity of the discharge coefficient to the main duct static pressure was reported in reference 1 at low pressure levels 7.4 to 25.0 psia (5.1 to 7.2 N/cm^2).

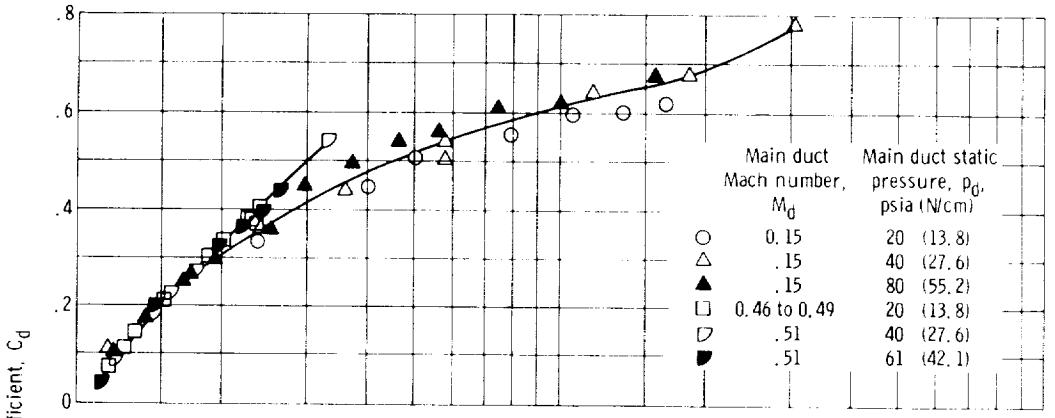

(a) Wall thickness to orifice diameter ratio, 0.51; model 1.

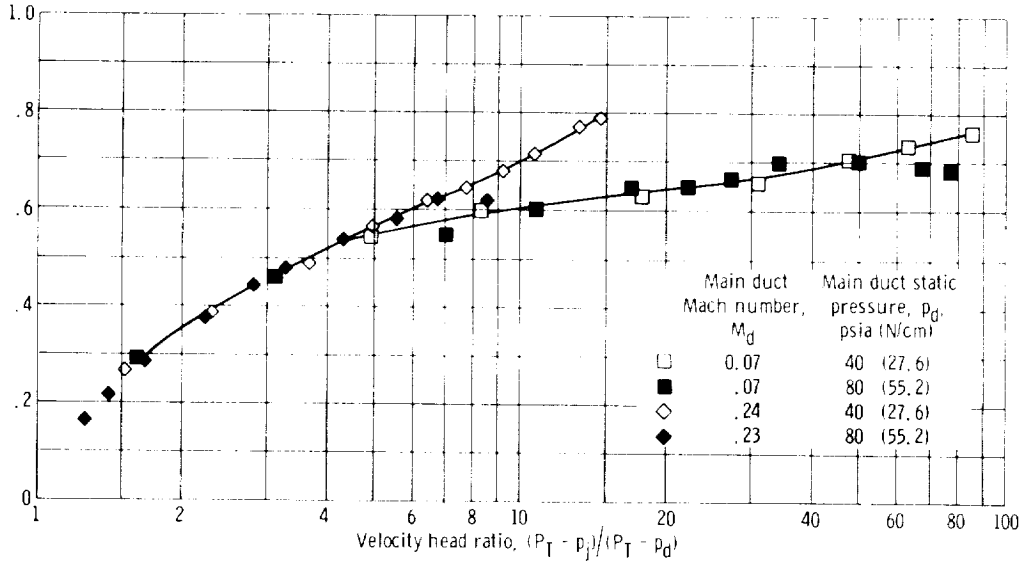

(b) Wall thickness to orifice diameter ratio, 1.05; model 3.

Figure 13. - Effect of varying orifice inlet pressure level on discharge coefficient for several main duct Mach numbers.

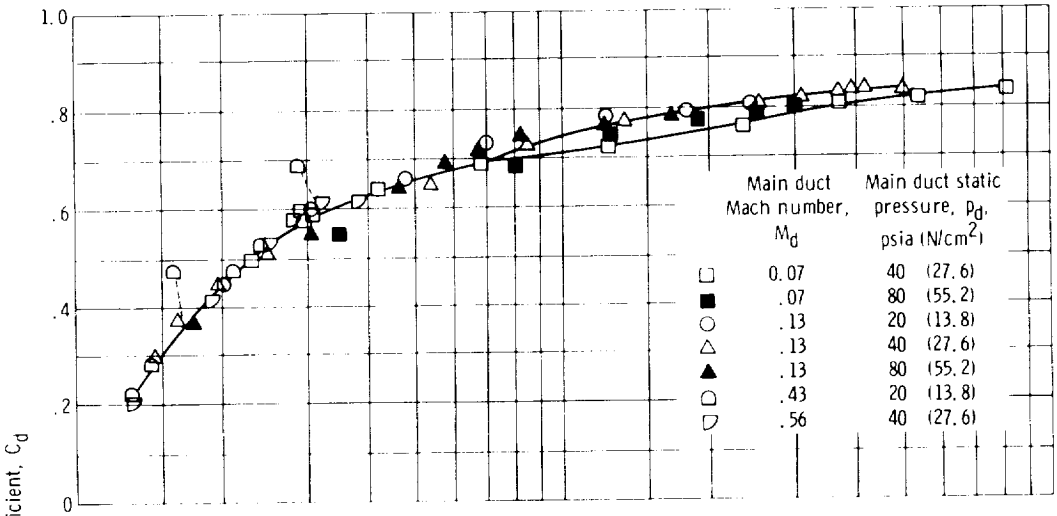

(c) Wall thickness to orifice diameter ratio, 2.00; model 5.

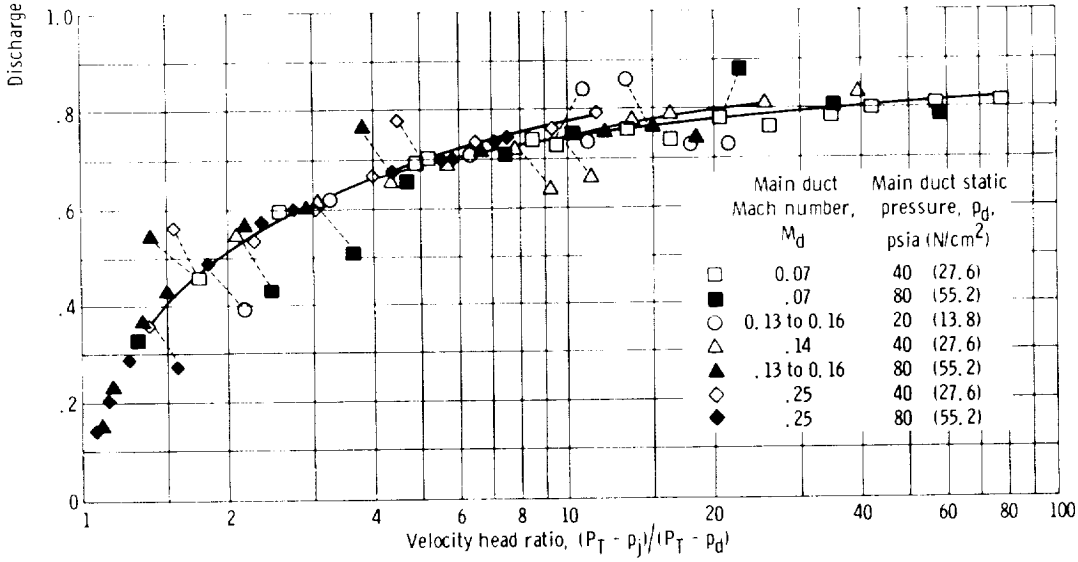

(d) Wall thickness to orifice diameter ratio, 4.00; model 7.

Figure 13. - Concluded.

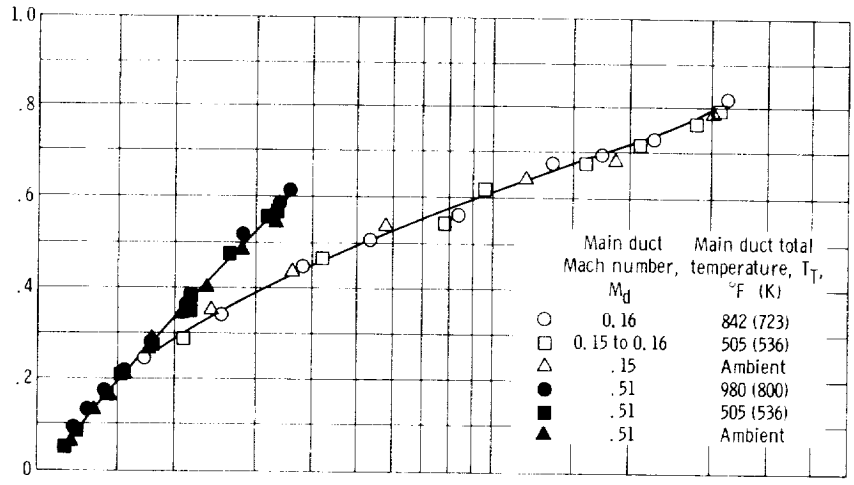

(a) Wall thickness to orifice diameter ratio, 0.51; model 1.

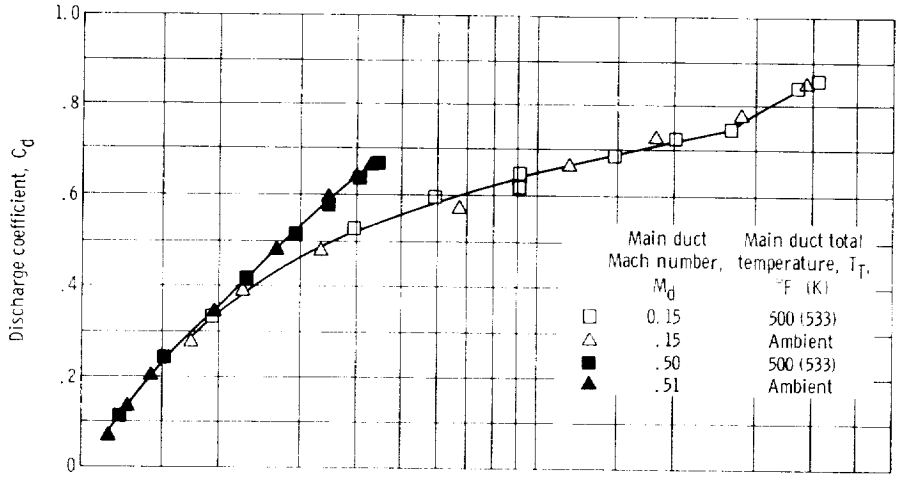

(b) Wall thickness to orifice diameter ratio, 1.02; model 2.

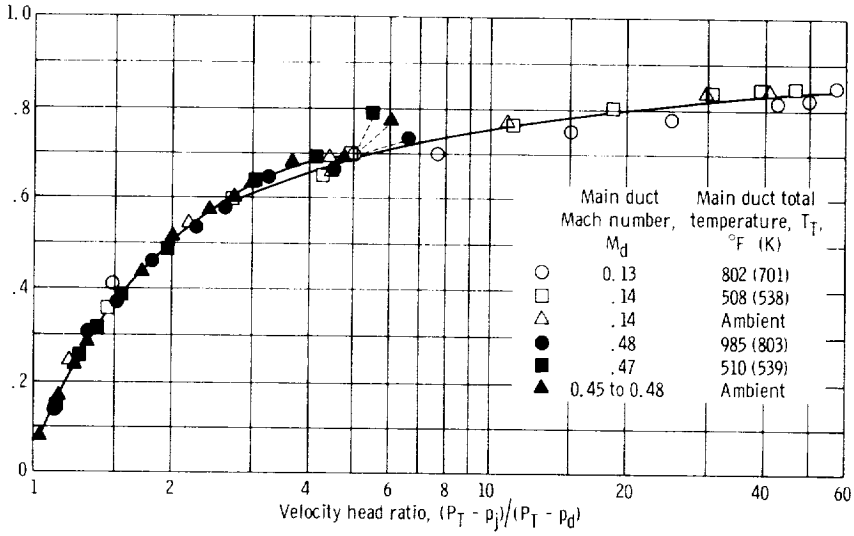

(c) Wall thickness to orifice diameter ratio, 2.83; model 6.

Figure 14. - Total air temperature effect on discharge coefficient for several main duct Mach numbers.

Temperature Effect

Increasing the main gas total temperature from ambient to approximately 1000° F (811 K), produced negligible variation in the discharge coefficient as seen in figure 14. Figure 14(c) shows a slight decrease in the discharge coefficient for the 800° F (700 K) case at a main duct Mach number of 0.14. This variation in the discharge coefficient with temperature could be the result of the increase in the air viscosity. The increase in viscosity would cause an increased pressure drop through the orifice for the same flow rate. The larger pressure differential would produce a larger ideal flow and a lower discharge coefficient. The variation in discharge coefficient due to temperature should be indicated on the high orifice flow portion (high velocity head ratio) of the curves through long orifices. The data presented in figure 14(c) is for the orifice with the largest t/d ratio run with high temperature air.

The true diameter of the orifice will increase as the tube walls heat up. The true orifice diameter will depend on the relative thermal strains throughout the model. The maximum possible diameter, which takes into account the variation in air temperature, was employed in the calculations. The thermal expansion of the orifice at 1000° F (811 K) total temperature, was approximately 0.0005 inch (0.0013 cm) on a 0.060 inch (0.152 cm) diameter. This value is equivalent to half the accuracy of measuring the orifice diameter.

Entrance Length Effects

The flow through the orifice with the approaching flow perpendicular to the orifice axis, occurs at the tube wall through the boundary layer. Figure 7(c) shows that the developing boundary layer has no appreciable influence on the discharge coefficient of an orifice after an entrance length of two diameters for an orifice with t/d equal to 2.00. Reference 1 showed this same lack of influence of the boundary layer for orifices of t/d ratios of 0.16 and 0.32.

Effect of an Orifice Surface Finish

Figure 15 shows the results of testing eight models, four each, of two different t/d ratios. Eight models were used to give a fairly large sample size on which to determine variations. Comparing model 10 and the data of model 4, which had approximately the same t/d of 1.5, and comparing model 11 and the uncorrected data of model 1, which had approximately the same t/d of 0.5, indicates that the electrical discharge machined holes are discharging more flow at the higher velocity head ratios and less flow at the

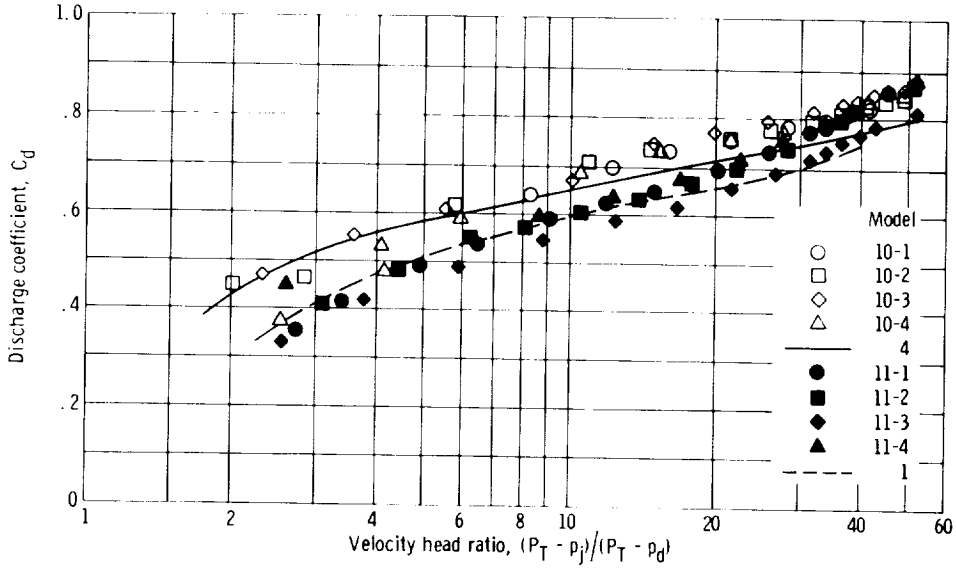

Figure 15. - Comparison of carefully made with electrical discharge machined orifices. A wall thickness to orifice diameter ratio of 1.49, model 10 is compared with model 4; and a wall thickness to orifice diameter ratio of 0.52, model 11 is compared with model 1. Main duct Mach number, 0.14.

lower velocity head ratios. The machining took place from the outside of the tube inward, which produced a radius or sometimes a burr on the inlet edge of the orifice (when viewed at 30 times magnification). The inlet radius could produce the increased discharge coefficient and the burr may account for the decrease in discharge coefficient shown. For design purposes the above variations can be neglected.

Orifice Interference Effects

Figure 16 shows a comparison of discharge coefficients for a single orifice t/d = 1.05 (model 3) with those of model 12 which had two identical orifices in tandem and spaced 1.5 orifice diameters apart. The data for the tandem orifices were obtained by averaging the discharge flow between the two orifices. At this spacing and t/d ratio, the interference effects can be considered negligible.

Method of Data Utilization

The method utilized to apply the data presented in this report is illustrated in the appendix.

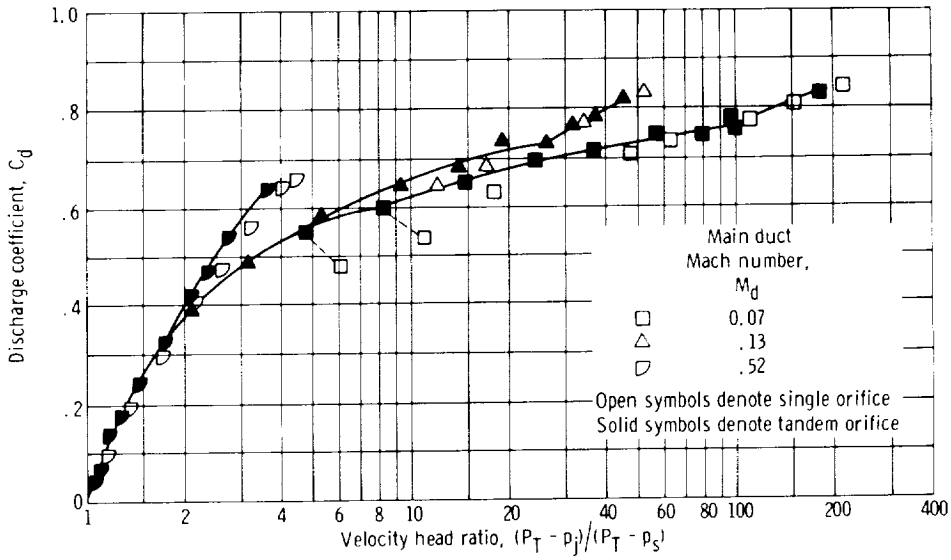

Figure 16. - Comparison of discharge coefficients for models with one orifice and two orifices in tandem. Model 3 (t/d = 1.05) and model 12 (t/d = 1.00 and spacing = 1.5 orifice diam).

SUMMARY OF RESULTS

From this investigation of the discharge coefficient for thick plate orifices with approach flow perpendicular or inclined to the orifice axis, the following results were obtained:

1. The main duct approach Mach number, static pressure differential across the orifice, the ratio of wall thickness to orifice diameter, and the inlet orifice edge radius were the predominant factors affecting the flow through the orifice.

2. Slanting the orifice axis in the direction of flow significantly increases the discharge coefficient.

3. Main duct wall curvature produced a small effect on the discharge coefficient.

4. The longitudinal interference of multiple orifices is not significant above an orifice center distance to orifice diameter ratio of 1.5 for an orifice with a wall thickness to orifice diameter ratio of 1.

5. Main duct air temperature and pressure level, entrance length, and orifice surface finish produced negligible effects on the discharge coefficient.

Lewis Research Center,
National Aeronautics and Space Administration,
Cleveland, Ohio, June 26, 1969,
720-03-00-79-22.

APPENDIX - METHOD OF DATA UTILIZATION

The discharge coefficient data presented in this report can be applied to either the evaluation or design of turbine blade coolant transfer holes or impingement holes. The data can be strictly applied only to the case of a thick plate orifice with the approaching flow perpendicular to the orifice axis. However, the results of reference 4 indicates that these data can be applied to the case of a thick plate orifice with both inlet and exit velocities with certain restrictions. Reference 4 concluded that, for low exit velocities perpendicular to the orifice and high jet velocities, the effect of exit flow velocity can be eliminated by calculation of a revised exit jet discharge pressure. The revised exit jet discharge static pressure is calculated by reducing the flow area of the exit duct passage by the width of the jet multiplied by the duct height. The high exit velocity case could be approximated by using the data in this report in conjunction with the data of references 5 and 6. The approximation would cover the orifices with a t/d greater than 1.0 or where the jet is attached on exit. By considering the inlet and exit velocities as two independent parameters, the discharge coefficient with the inlet velocity can be obtained from the data presented in this report and then corrected for the exit velocity using the data presented in references 5 (fig. 7(a)) and 6 (fig. 6(c)).

The use of curves presented in this report requires that the total and static pressures in the inlet passage and the exit jet static pressure be known. These values of pressure could be obtained by experimental measurements or by calculation in some cases, provided the mass flow rates and required flow areas are available. Cases where the major portion of the jet velocity head is recovered, as in the leading edge of an impingement blade or vane, require experimental measurements of the exit jet static pressure.

The evaluation of the flow through a given turbine blade cooling air transfer hole or impingement hole can be accomplished as follows:

(1) Determine the appropriate curve of discharge coefficient against the velocity head ratio based on the existing orifice and main duct geometry.

(2) Calculate the velocity head ratio $(P_T - p_j)/(P_T - p_d)$, and the approach flow Mach number M_d.

(3) Determine the discharge coefficient from the curve selected in (1) at the appropriate values of velocity head ratio and approach flow Mach number.

(4) Calculate the ideal jet velocity and density using equations (2) and (3), respectively.

(5) Determine the actual flow through the orifice from equation (1).

The design of a given turbine blade transfer hole or impingement hole to pass a specified quantity of flow can be accomplished as follows:

(1) Calculate the velocity head ratio $(P_T - p_j)/(P_T - p_d)$, and the approach flow Mach number, M_d.

(2) Assume a nominal wall thickness to orifice diameter ratio, for example 1.6.

(3) Determine the discharge coefficient from the curve of discharge coefficient against the velocity head ratio (shown in fig. 8) if the approach flow Mach number is 0.13. Figure 5 or 7 must be utilized or a figure similar to figure 8 plotted for the other approach flow Mach numbers.

(4) Calculate the jet velocity and density using equations (2) and (3), respectively.

(5) Determine the diameter of the orifice required to give the area obtained from equation (1).

(6) Compare this diameter with the t/d ratio selected in step (2) to determine the wall thickness.

(7) If the wall thickness or diameter is unreasonable, select a new t/d ratio and return to step (2).

This design procedure applies only to the cases where the exit jet pressure can be calculated.

The methods presented illustrate the procedure for handling the cases that closely simulate the exact model geometries. Corrections to these procedures to account for effects like main duct wall curvature, placing the orifice on an angle, and inlet edge conditions may be necessary. The wall curvature variation could be extrapolated from figure 12 to figures 5 and 7 with reasonable confidence. The variation of placing the orifice on an angle or the inlet edge condition have such a marked effect on discharge coefficient, that its extrapolation to t/d ratios other than 1.0 would be questionable.

REFERENCES

1. Dittrich, Ralph T.; and Graves, Charles C.: Discharge Coefficients for Combustor-Liner Air-Entry Holes. I - Circular Holes with Parallel Flow. NACA TN 3663, 1956.

2. Stokes, George M.; Davis, Don D., Jr.; and Sellers, Thomas B.: An Experimental Study of Porosity Characteristics of Perforated Materials in Normal and Parallel Flow. NACA TN 3085, 1954.

3. Seglem, Clifford E.: The Discharge Coefficient of a Combustor Air Inlet Hole. M. S. Thesis, Univ. of Pittsburgh, 1952.

4. Callaghan, Edmund E.; and Bowden, Dean T.: Investigation of Flow Coefficient of Circular, Square, and Elliptical Orifices at High Pressure Ratios. NACA TN 1947, 1949.

5. Dewey, Paul E.: A Preliminary Investigation of Aerodynamic Characteristics of Small Inclined Air Outlets at Transonic Mach Numbers. TN 3442, 1955.

6. Nelson, William J.; and Dewey, Paul E.: A Transonic Investigation of the Aerodynamic Characteristics of Plate- and Bell-Type Outlets for Auxilliary Air. NACA RM L52H20, 1952.

7. Dittrich, Ralph T.: Discharge Coefficients for Combustor-Liner Air-Entry Holes. II - Flush Rectangular Holes, Step Louvers, and Scoops. NACA TN 3924, 1958.

8. Shapiro, Ascher H.: The Dynamics and Thermodynamics of Compressible Fluid Flow. Ronald Press Co., 1953.

9. Perry, J. A., Jr.: Critical Flow Through Sharp-Edged Orifices. Trans. ASME, vol. 71, no. 7, Oct. 1949, pp. 757-764.

10. Lichtarowicz, A.; Duggins, R. K.; and Markland, E.: Discharge Coefficients for Incompressible Non-Cavitating Flow Through Long Orifices. J. Mech. Eng. Sci., vol. 7, no. 2, June 1965, pp. 210-219.

NASA-Langley, 1969 —— 12 **E-5119**

NATIONAL AERONAUTICS AND SPACE ADMINISTRATION
WASHINGTON, D.C. 20546

OFFICIAL BUSINESS

FIRST CLASS MAIL

POSTAGE AND FEES PAID
NATIONAL AERONAUTICS AND
SPACE ADMINISTRATION

POSTMASTER: If Undeliverable (Section 158 Postal Manual) Do Not Return

"The aeronautical and space activities of the United States shall be conducted so as to contribute . . . to the expansion of human knowledge of phenomena in the atmosphere and space. The Administration shall provide for the widest practicable and appropriate dissemination of information concerning its activities and the results thereof."

—NATIONAL AERONAUTICS AND SPACE ACT OF 1958

NASA SCIENTIFIC AND TECHNICAL PUBLICATIONS

TECHNICAL REPORTS: Scientific and technical information considered important, complete, and a lasting contribution to existing knowledge.

TECHNICAL NOTES: Information less broad in scope but nevertheless of importance as a contribution to existing knowledge.

TECHNICAL MEMORANDUMS: Information receiving limited distribution because of preliminary data, security classification, or other reasons.

CONTRACTOR REPORTS: Scientific and technical information generated under a NASA contract or grant and considered an important contribution to existing knowledge.

TECHNICAL TRANSLATIONS: Information published in a foreign language considered to merit NASA distribution in English.

SPECIAL PUBLICATIONS: Information derived from or of value to NASA activities. Publications include conference proceedings, monographs, data compilations, handbooks, sourcebooks, and special bibliographies.

TECHNOLOGY UTILIZATION PUBLICATIONS: Information on technology used by NASA that may be of particular interest in commercial and other non-aerospace applications. Publications include Tech Briefs, Technology Utilization Reports and Notes, and Technology Surveys.

Details on the availability of these publications may be obtained from:

SCIENTIFIC AND TECHNICAL INFORMATION DIVISION

NATIONAL AERONAUTICS AND SPACE ADMINISTRATION

Washington, D.C. 20546